



University
of Glasgow

Molla, M.M. and Paul, M.C. (2008) *LES of physiological pulsatile flow in a model arterial stenosis*. In: 4th BSME - ASME International Conference on Thermal Engineering, 27-29 December 2008, Dhaka, Bangladesh.

<http://eprints.gla.ac.uk/4911/>

Deposited on: 3 February 2009

LES OF PHYSIOLOGICAL PULSATILE FLOW IN A MODEL ARTERIAL STENOSIS

Md. Mamun Molla and Manosh C. Paul

Department of Mechanical Engineering, University of Glasgow, Glasgow G12 8QQ, UK
e-mail: m.paul@mech.gla.ac.uk

ABSTRACT

Physiological pulsatile flow in a 3D model of arterial stenosis is investigated by applying Large Eddy Simulation (LES) technique. The computational domain has been chosen is a simple channel with a biological type stenosis formed eccentrically on the top wall. The physiological pulsation is generated at the inlet of the model using the fourth harmonic of the Fourier series of the physiological pressure pulse. The flow Reynolds numbers which are typical of those found in human large artery are chosen in the present work. Transitions to turbulent of the pulsatile flow in the post stenosis are examined through the various numerical results and explained physically along with the relevant medical concerns.

KEYWORDS: *Arterial stenosis, LES, Physiological flow, Turbulent flow*

1 INTRODUCTION

The term arterial stenosis refers the narrowing of an artery where the cross-sectional area of blood vessel reduces. The most common cause is the atherosclerosis where cholesterol and other lipids are deposited beneath the intima (inner lining) of the arterial wall. As the amount of this fatty material increases there is an accompanying proliferation of connective tissue and the whole forms a thickened area in the vessel wall called plaque. The vessel wall remodels to accommodate this varying degrees but with marked plaque deposition then this will reduce the effective cross-section of the vessel and retard the blood flow. When the reduction in vessel calibre is severe the result is that blood flow transient to turbulent and there will be a pressure drop across the stenotic region.

The alteration in flow dynamics in turn produces abnormal wall shear stress both at the plaque and at the post stenotic area such that the plaque may fissure and rupture exposing the lipid plaque core to the blood stream with potential for thrombosis (blood clotting) at the site of rupture. This development of atherothrombosis may dangerously acutely occlude the vessels with in critical territories such as the coronary arteries and cerebral vessels catastrophic results. Non-occlusive atherothrombosis is also clinically important as the thrombotic material deposited is often unstable and a source of distal embolism, this is particularly important in the extracranial carotid arteries as a source of stroke.

The blood flow through arteries is inherently unsteady due to the cyclic nature of heart pump. These disturbed flows may either be laminar or transition to turbulent and the pulsatile character of the flow has a significant effect on the transition to turbulence which represents an abnormal flow nature in the circulation, and the development of transition to turbulence flow in the arteries has a clinical interest as outlined above. From the point of an accurate computational modelling, such flow can be challenging.

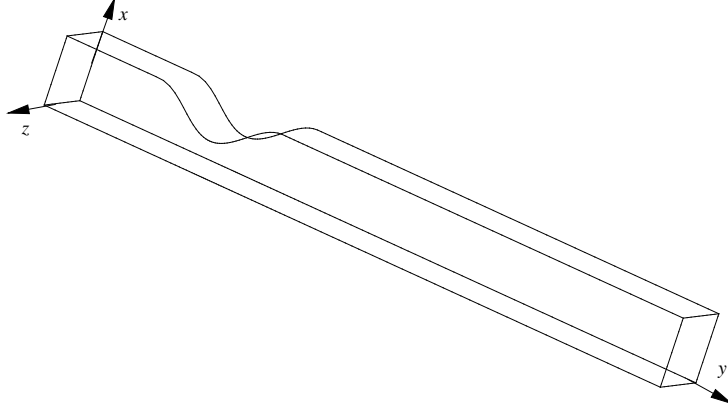


Figure 1: A schematic of the model with coordinate system.

Very recently Paul *et al.* [1] have investigated the non-additive pulsatile turbulent blood flow through a model of arterial stenosis applying the LES technique. Using the first harmonic of the Fourier series of the pressure pulse, a Large-eddy simulation of the physiological pulsatile flow in the same model is performed by Molla *et al.* [2]. In the present paper, the aim is to use more accurate pulsatile inflow and investigate the turbulent flow downstream of the stenosis applying the LES. In this regard, the fourth harmonic of the Fourier series of the physiological pressure pulse (Womersley [3]) is used in the model. The results obtained by LES are compared with those of Direct Numerical Simulation (DNS). The fluid in the model is treated as Newtonian and incompressible according to Pedley [4].

2 FORMATION OF THE PROBLEM

2.1 Model geometry

The geometry shown in Fig. 1 consists of a 3D channel with one sided cosine shape stenosis on the upper wall centred at $y/L = 0.0$, where y is the horizontal distance or the distance along the flow and L is the height of the channel. In the model the height (x) and its width (z) are kept same, which gives a square cross-section at the upstream and downstream of the stenosis. The length of the stenosis is equal to twice of the channel height. Before the stenosis the channel length is $5L$, and $15L$ is the downstream region of the stenosis.

2.2 Governing equations for LES

The equations of motion for Large Eddy Simulation are obtained by applying a spatial filter, namely *grid*-filter, to the Navier-Stokes equations and written in the following filtered forms:

$$\frac{\partial \bar{u}_j}{\partial x_j} = 0, \quad (1)$$

$$\frac{\partial \bar{u}_j}{\partial t} + \frac{\partial \bar{u}_i \bar{u}_j}{\partial x_j} = -\frac{1}{\rho} \frac{\partial \bar{P}}{\partial x_i} + \frac{\partial}{\partial x_j} \left[\nu \left(\frac{\partial \bar{u}_i}{\partial x_j} + \frac{\partial \bar{u}_j}{\partial x_i} \right) \right] - \frac{\partial \tau_{ij}}{\partial x_j}, \quad (2)$$

where \bar{u}_i is the velocity vector along $x_i = (x, y, z)$, \bar{P} is pressure, t is time, ρ is the fluid density, and ν is the kinematic viscosity of the fluid. The effects of the small scale appear in the subgrid-scale stress (SGS) term as

$$\tau_{ij} = \overline{u_i u_j} - \bar{u}_i \bar{u}_j, \quad (3)$$

which is modelled as (Smagorinsky [5]),

$$\tau_{ij} - \frac{1}{3}\delta_{ij}\tau_{kk} = -2(C_s\Delta)^2|\bar{S}|\bar{S}_{ij}, \quad (4)$$

where $\Delta = \sqrt[3]{\Delta x \Delta y \Delta z}$ is the filter width and $|\bar{S}| = \sqrt{2\bar{S}_{ij}\bar{S}_{ij}}$ is the magnitude of the large scale strain rate tensors defined as $\bar{S}_{ij} = \frac{1}{2}\left(\frac{\partial \bar{u}_i}{\partial x_j} + \frac{\partial \bar{u}_j}{\partial x_i}\right)$. The unknown Smagorinsky constant, C_s , is calculated using the localized dynamic model of Piomelli and Liu [6].

2.3 Boundary conditions

To generate the physiological pulsatile flow at the inlet of the model artery, one-dimensional form of the Navier-Stokes equation (2) for the streamwise velocity is solved first taking the pressure gradient as a Fourier series in time (Womersley [3], Loudon and Tordesillas [7]),

$$-\rho\frac{\partial \bar{v}}{\partial t} + \mu\frac{\partial^2 \bar{v}}{\partial x^2} = \frac{2}{3}A_0 + A\sum_{n=1}^N M_n e^{i(n\omega t + \phi_n)}, \quad (5)$$

where A_0 and A are the constants corresponding to the steady and oscillatory pressure gradient respectively; M_n and ϕ_n are the respective coefficients and the phase angle of the different harmonics, which are known from Womersley [3]; N is the number of harmonics of the Fourier series; and $\omega = \frac{2\pi}{T}$ is the frequency of the unsteady flow. The solution of Eq. (5) takes the following form:

$$\bar{v}(x, t) = 4\bar{V}\frac{x}{L}\left(1 - \frac{x}{L}\right) + A\sum_{n=1}^N \frac{iM_n L^2}{\mu\omega_0^2 n} \left[\cosh(\omega_0\sqrt{in}\frac{x}{L}) - \frac{\cosh(\omega_0\sqrt{in}) - 1}{\sinh(\omega_0\sqrt{in})} \sinh(\omega_0\sqrt{in}\frac{x}{L}) - 1 \right] e^{i(n\omega t + \phi_n)}. \quad (6)$$

The real part of this solution is used as the inlet condition to generate the physiological velocity profiles. We have used $N = 4$ (fourth harmonic) in the simulation. In Eq. (6), the bulk velocity \bar{V} relates to the flow Reynolds number defined as $Re = \frac{\bar{V}L}{\nu}$, and $\omega_0 = L\sqrt{\frac{\rho\omega}{\mu}}$ is the Womersley number. In Fig. 2, the inlet velocity profile is presented for one pulsation for $Re = 2000$ and $\omega_0 = 10.5$, note that the velocity in frame (a) is recorded at very close to the bottom wall. The choice of the Womersley number of 10.5 in the simulation indicates that the unsteady part of the velocity dominates the flow, see Ku [8]. In addition, the maximum streamwise velocity at the inlet is controlled by taking the value of the amplitude of oscillation as $A = 0.4$.

No slip boundary conditions are used for both the lower and upper walls of the model, and at the outlet a convective boundary condition is used. For the spanwise boundaries, periodic boundary conditions are applied for modelling the spanwise homogeneous flow.

2.4 Overview of the numerical procedures

The governing filtered equations (1-2) in Cartesian coordinates are transformed into curvilinear coordinates system and the finite volume approaches are used to discretise the partial differential equations to yield a system of linear algebraic equations. To discretise the spatial derivatives in eqns. (1-2), the standard second order accurate central difference scheme is used, except for the convective terms in the momentum equations (2) for which an energy conserving discretisation scheme is used.

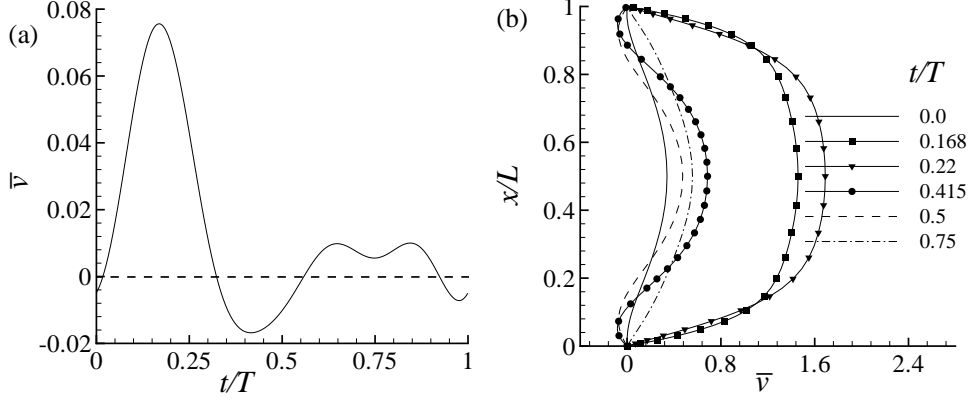


Figure 2: Streamwise velocity at the inlet for $Re = 2000$ and $\omega_0 = 10.5$.

Time derivatives are discretised by a three point backward difference scheme with a constant timestep of $\delta t = 10^{-3}$. A pressure correction algorithm is applied to couple pressure with the velocity components where the results are stored at the centre of a control volume according to the collocated grid arrangement. The Poisson like pressure correction equation is discretised by using the pressure smoothing approach of Rhie and Chow [9], which prevents the even-odd node uncoupling in the pressure and velocity fields.

A BI-CGSTAB [10] solver is used for solving the matrix of velocity vectors, while for the Poisson like pressure correction equation a ICCG [11] solver is applied due to its symmetric and positive definite nature. Overall the code is second order accurate in both time and space and fully implicit, which is in-house developed and has been applied extensively in other engineering flows.

The methods of data processing for the random turbulent fluctuations and the spanwise average quantities are summarised in Molla and Paul [12].

3 RESULTS AND DISCUSSION

In the present study the Reynolds numbers ranging from 1000 to 2000 are chosen for simulation, and the area reduction of the channel due to the stenosis is fixed at 50%. The numerical grid employed in the LES consists of a total of 5×10^5 control volumes with $50 \times 200 \times 50$ grid nodes in the x and y and z directions respectively. A finer grid of $70 \times 350 \times 50$ has been employed in the DNS for $Re = 2000$ and the results are compared with those of LES. The statistics for mean quantities have been gathered after finishing the ten cycles of the pulsation, where the mean flow eventually becomes stationary.

The streamwise mean streamlines based on the mean velocity components, $\langle \bar{u} \rangle$ and $\langle \bar{v} \rangle$, are depicted in Fig. 3 while $Re = 2000$. It is seen that a re-circulating region is created after the stenosis near the upper wall owing to the experience of the adverse pressure gradient in this region. The blood flow in this recirculation region stays for a long time, and this prolonging staying time is known to be an important factor for causing the heart attack or brain stroke to a patient suffering from a disease related to arterial stenosis. Figure 4 shows the contours of the spanwise-averaged vorticity, $\omega_z = \frac{\partial \bar{u}}{\partial y} - \frac{\partial \bar{v}}{\partial x}$, for $Re = 2000$ when the pulsation attains its peak position. It can be seen in this figure that the two shear layers, one of which separating from the nose of the stenosis generates an anticlockwise (dashed lines) vortex close to the lip region, while the other one separating from the bottom wall induces a clockwise (solid lines) vortex in the post-stenosis. These pair vortices then interact and create highly oscillating flow at the downstream of the

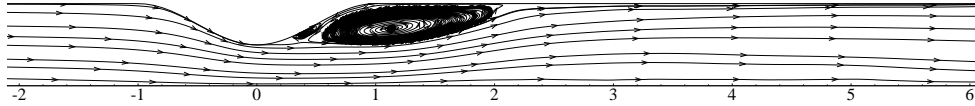


Figure 3: Mean streamlines while $Re = 2000$.

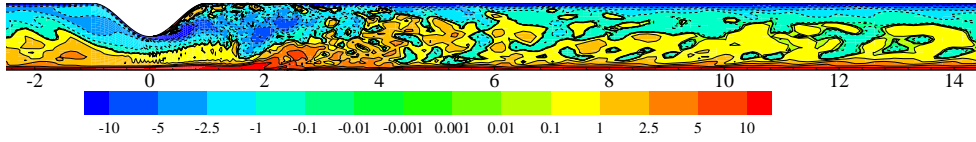


Figure 4: Spanwise-averaged vorticity while $Re = 2000$.

stenosis. The instantaneous shear stress distributions, $\tau_{xy} = \mu \left(\frac{\partial \bar{u}}{\partial y} + \frac{\partial \bar{v}}{\partial x} \right)$, at the upper wall is shown in Figure 5 for the different Reynolds numbers. Just prior to the centre of the stenosis, an acute stress drop happens due to the flow separation. This low shear stress usually stimulates the growth of tissue proliferation at the throat of the stenosis, and as a result the reduction of the arterial area increases, which might be a severe condition for a patient. The oscillatory stresses in the post-stenosis are also a concerned matter in the point of pathological view as these could smash up the material of the blood cells as well as the inner lining of an artery.

Figure 6 shows the mean pressure, $\langle \bar{p} \rangle$, at the upper wall. It is very much clear in this figure that the maximum pressure drop occurs at the centre of the stenosis, which is located at the region $0 \leq y/L \leq 2.0$ and this is the region where the flow re-circulating region was found (see Fig. 3). Finally, Fig. 7 illustrates the normalised turbulent kinetic energy (TKE) for the different Reynolds numbers. Before the stenosis the TKE is very small, which is expected, as the pulsatile flow is laminar; but after the centre of stenosis in the post-stenosis region, $0 < y/L < 5$, the high levels of TKE usually play a significant role in the formation of thrombosis by inducing platelet aggregation in blood.

4 CONCLUSION

Large Eddy Simulation with a localized dynamic sub-grid model has been applied to study the physiological pulsatile flow through a 3D model of arterial stenosis. In the model, the stenosis was placed eccentrically at the upper wall of the channel, which reduces the cross-sectional area of the channel of 50%. The different Reynolds numbers, 1000, 1400, 1700 and 2000, based on the bulk velocity, were chosen for this study – the

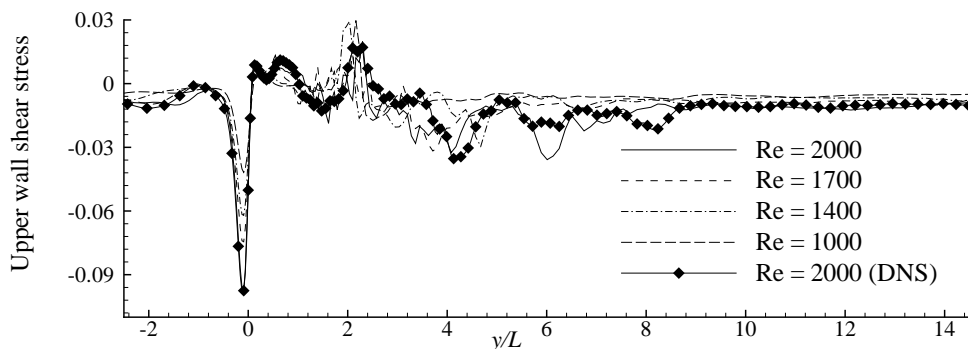


Figure 5: Instantaneous shear stress at the upper wall for the different Reynolds numbers.

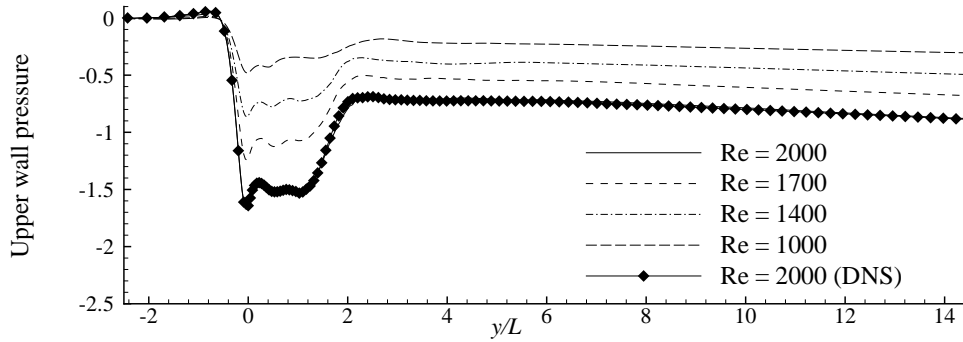


Figure 6: Mean pressure at the upper wall for the different Reynolds numbers.

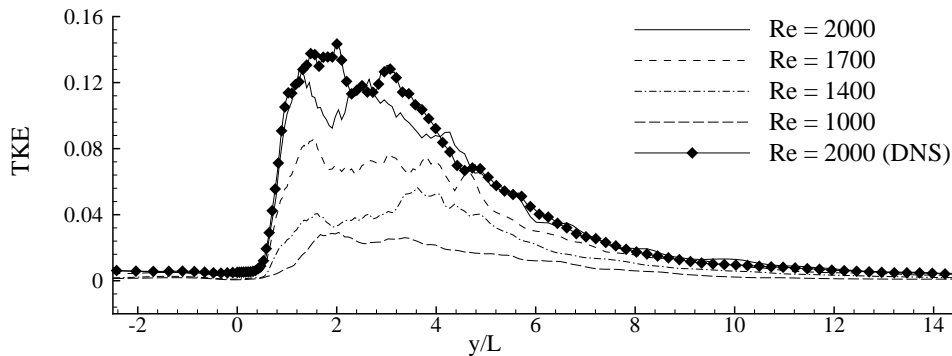


Figure 7: Turbulent kinetic energy for the different Reynolds numbers.

choice of these Reynolds numbers is realistic for human arteries, see Ku [8]. The results obtained by the LES have also been compared with those of the DNS for $Re = 2000$ and the agreement we found is quite satisfactory.

The turbulent kinetic energy is found high in the downstream of the stenosis because of the highly oscillating nature of the transient flow and the shear stresses in that region. As reported, the level of this turbulence has an impact in causing damage to the materials of blood cells and activate the blood platelets and, consequently, these could create many pathological diseases. Although a simple model is considered here, we believe that the results presented in the paper would give a better insight and in-depth knowledge to understand the important fluid dynamics roles of atherosclerosis. Future extension of this work is to consider a more biological realistic domain, e.g. circular domain, and investigate the turbulent flow coupling the fluid with structure.

Acknowledgements: The first author acknowledges gratefully the receipt of studentships from the Faculty of Engineering and ORSAS. Many thanks to Dr Roditi, consultant radiologist of Glasgow Royal Infirmary, for helpful discussions on the various clinical aspects of the results.

REFERENCES

- [1] M. C. Paul, M. M. Molla, G. Roditi, Large-eddy simulation of pulsatile blood flow, *Med. Eng. Phys.* (in press) doi:10.1016/j.medengphy.2008.04.014.
- [2] M. M. Molla, M. C. Paul, G. Roditi, Physiological flow in a model of arterial stenosis, *J. Biomech.* 41(S1) (2008) S243.

- [3] J. R. Womersley, Method for the calculation of velocity, rate of flow and viscous drag in arteris when the pressure gradient is known, *J. Physiol.* 155 (1955) 553–563.
- [4] T. J. Pedley, *The fluid mechanics of large blood vessels*, Cambridge University Press, 1980.
- [5] J. Smagorinsky, General circulation experiment with the primitive equations. i. the basic experiment, *Monthly Weather Rev.* 91 (1963) 99–164.
- [6] U. Piomelli, J. Liu, Large-eddy simulation of rotating channels flows using a localized dynamic model, *Phys. Fluids* 7 (4) (1994) 839–847.
- [7] C. Loudon, A. Tordesillas, The use of the dimensionless Womersley number to characterize the unsteady nature of internal flow, *J. Theo. Biol.* 191 (1998) 63–78.
- [8] D. N. Ku, Blood flows in arteries, *Annu. Rev. Fluid Mech.* 29 (1997) 399–434.
- [9] C. M. Rhie, W. L. Chow, Numerical study of the turbulent flow past an airfoil with trailing edge separation, *AIAA J.* 21(11) (1983) 1525–1532.
- [10] H. A. D. Vorst, BI-CGSTAB: a first and smoothly converging variant of BI-CG for the solution of the non-symmetric linear systems, *SIAM J. Sci. Stat. Comput.* 13 (2) (1992) 631–644.
- [11] D. S. Kershaw, The Incomplete Cholesky-Cojugate Gradient method for the iterative solution of systems, *J. Com. Phys.* 26 (1978) 43–65.
- [12] M. M. Molla, M. C. Paul, A study of transition to turbulent pulsatile flow in a model arterial stenosis using large eddy simulation, *Comp. and Fluids.* (2008) submitted.